Prospects for $\gamma\gamma \to$ Higgs observation in ultraperipheral ion collisions at the Future Circular Collider

David d'Enterria[1], *Daniel E. Martins*[2], *and Patricia Rebello Teles*[3]
[1]CERN, EP Department, 1211 Geneva.
[2]UFRJ, Univ. Federal do Rio de Janeiro, 21941-901, Rio de Janeiro, RJ.
[3]CBPF, Centro Brasileiro de Pesquisas Físicas, 22290-180, Rio de Janeiro, RJ.

Abstract
We study the two-photon production of the Higgs boson, $\gamma\,\gamma \to$ H, at the Future Circular Collider (FCC) in ultraperipheral PbPb and pPb collisions at $\sqrt{s_{\rm NN}} = 39$ and 63 TeV. Signal and background events are generated with MADGRAPH 5, including γ fluxes from the proton and lead ions in the equivalent photon approximation, yielding $\sigma(\gamma\,\gamma \to {\rm H})$ = 1.75 nb and 1.5 pb in PbPb and pPb collisions respectively. We analyse the H$\to b\bar{b}$ decay mode including realistic reconstruction efficiencies for the final-state b-jets, showered and hadronized with PYTHIA 8, as well as appropriate selection criteria to reduce the $\gamma\,\gamma \to b\bar{b}, c\bar{c}$ continuum backgrounds. Observation of PbPb$\xrightarrow{\gamma\gamma}$(Pb)H(Pb) is achievable in the first year with the expected FCC integrated luminosities.

Keywords
Higgs boson; two-photon fusion; heavy-ion collisions; CERN; FCC.

1 Introduction

The observation of the predicted Higgs boson [1] in proton-proton collisions at the Large Hadron Collider [2, 3] has represented a breakthrough in our scientific understanding of the particles and forces in nature. A complete study of the properties of the scalar boson, including its couplings to all known particles, and searches of possible deviations indicative of physics beyond the Standard Model (SM), require a new collider facility with much higher center-of-mass (c.m.) energies [4]. The Future Circular Collider (FCC) is a post-LHC project at CERN, aiming at pp collisions up to at a c.m. energy of $\sqrt{s} = 100$ TeV in a new 80–100 km tunnel with 16–20 T dipoles [5]. The FCC running plans with hadron beams (FCC-hh) includes also heavy-ion operation at nucleon-nucleon c.m. energies of $\sqrt{100}$ TeV$.\sqrt{Z_1 Z_2/(A_1 A_2)} = 39$ TeV, 63 TeV for PbPb, pPb with (monthly) integrated luminosities of 110 nb^{-1} and 29 pb^{-1} [6]. Such high collision energies and luminosities, factors of 7 and 30 times higher respectively than those reachable at the LHC, open up the possibility to study the production of the Higgs boson in nuclear collisions, both in central hadronic [7] as well as in ultraperipheral (electromagnetic) [8] interactions. The observation of the latter $\gamma\,\gamma \to$ H process provides an independent measurement of the H-γ coupling not based on Higgs decays but on its s-channel production mode.

The measurement of exclusive $\gamma\,\gamma \to$ H in ultraperipheral collisions (UPCs) [9, 10] of pPb and PbPb beams was studied in detail for LHC energies[1] in [8], although its observation there is unfeasible with the nominal luminosities (Fig. 1, left). We extend such studies for FCC energies, where such an observation is warranted. All charges accelerated at high energies generate electromagnetic fields which, in the equivalent photon approximation (EPA) [12], can be considered as quasireal photon beams[2] [13]. The highest available photon energies are of the order of the inverse Lorentz-contracted radius R of the source charge, $\omega_{\rm max} \approx \gamma/R$, which at the FCC yield photon-photon collisions above 1 TeV (Table 1). In

[1]A few older papers had already previously discussed the possibility to produce the Higgs boson in heavy-ion UPCs [11].
[2]The emitted photons are almost on mass shell, with virtuality $-Q^2 < 1/R^2$, where R is the radius of the charge, i.e. $Q \approx 0.28$ GeV for protons ($R \approx 0.7$ fm) and $Q < 0.06$ GeV for nuclei ($R_A \approx 1.2\,A^{1/3}$ fm) with mass number $A > 16$.

https://doi.org/10.23727/CERN-Proceedings-2018-001.33

addition, since the photon flux scales as the squared charge of the beam, Z^2, two-photon cross sections are enhanced millions of times for ions ($Z^4_{\rm Pb}$ = 5·10^7 for PbPb) compared to proton or electron beams, thereby featuring the largest $\gamma\,\gamma$ luminosities among all colliding systems (Fig. 1, left).

Table 1: Relevant parameters for photon-photon processes in ultraperipheral pPb and PbPb collisions at the FCC: (i) nucleon-nucleon c.m. energy, $\sqrt{s_{\rm NN}}$, (ii) integrated luminosity per year, $\mathcal{L}_{\rm int}$, (iii) beam energies, $\rm E_{beam}$, (iv) Lorentz factor, $\gamma = \sqrt{s_{\rm NN}}/(2\,m_N)$, (v) effective (Pb) radius, R_A, (vi) photon "cutoff energy" in the c.m. frame, $\omega_{\rm max}$, and (vii) "maximum" photon-photon c.m. energy, $\sqrt{s^{\rm max}_{\gamma\,\gamma}}$. The last column lists the $\gamma\,\gamma \to$ H cross sections.

System	$\sqrt{s_{\rm NN}}$	$\mathcal{L}_{\rm int}$	$E_{\rm beam1} + E_{\rm beam2}$	γ	R_A	$\omega_{\rm max}$	$\sqrt{s^{\rm max}_{\gamma\,\gamma}}$	$\sigma(\gamma\gamma \to {\rm H})$
pPb	63 TeV	29 pb^{-1}	50. + 19.5 TeV	33 580	7.1 fm	950 GeV	1.9 TeV	1.5 pb
PbPb	39 TeV	110 nb^{-1}	19.5 + 19.5 TeV	20 790	7.1 fm	600 GeV	1.2 TeV	1.75 nb

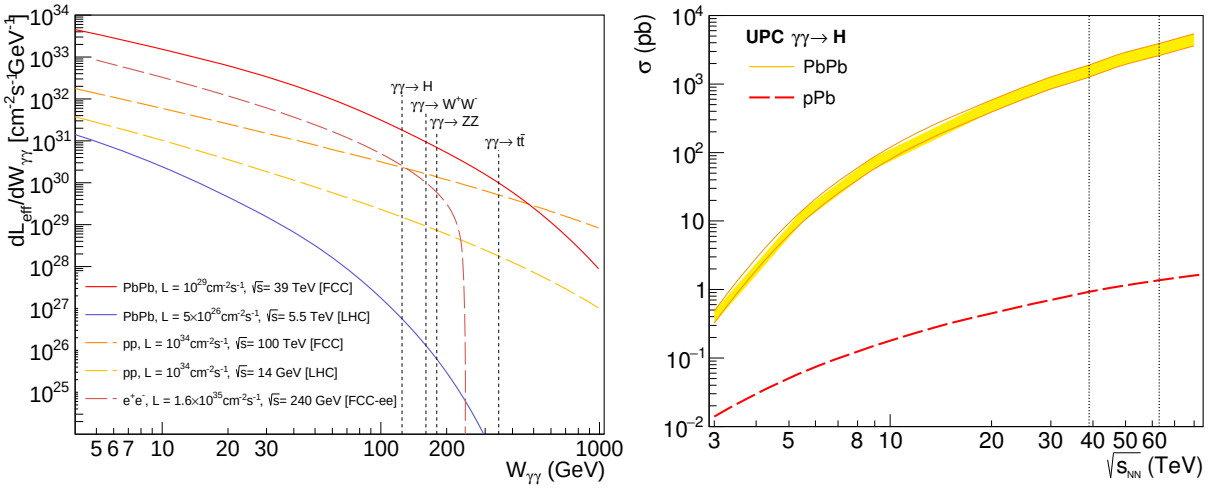

Fig. 1: Left: Two-photon effective luminosities as a function of $\gamma\,\gamma$ c.m. energy over $W_{\gamma\,\gamma} \approx$ 5–1000 GeV in PbPb, pp, and e^+e^- collisions at the FCC [5, 6, 14], and in PbPb and pp collisions at the LHC. Right: Two-photon fusion Higgs boson cross section versus nucleon-nucleon c.m. energy in ultraperipheral PbPb (top) and pPb (bottom curve) collisions. The vertical lines indicate the expected FCC running energies at $\sqrt{s_{\rm NN}}$ = 39 and 63 TeV.

2 Theoretical setup

The MADGRAPH 5 (v.2.5.4) [15] Monte Carlo (MC) event generator is used to compute the relevant cross sections from the convolution of the Weizsäcker-Williams EPA photon fluxes [12] for the proton and lead ion, and the H-γ coupling parametrized in the Higgs effective field theory [16], following the implementation discussed in [8] with a more accurate treatment of the non hadronic-overlap correction. The proton γ flux is given by the energy spectrum $f_{\gamma/p}(x)$ where $x = \omega/E$ is the fraction of the beam energy carried by the photon [17]:

$$f_{\gamma/p}(x) = \frac{\alpha}{\pi}\,\frac{1 - x + 1/2x^2}{x}\int_{Q^2_{\rm min}}^{\infty}\frac{Q^2 - Q^2_{\rm min}}{Q^4}|F(Q^2)|^2 dQ^2\,, \tag{1}$$

with $\alpha = 1/137$, $F(Q^2)$ the proton electromagnetic form factor, and the minimum momentum transfer $Q_{\rm min}$ is a function of x and the proton mass m_p, $Q^2_{\rm min} \approx (x m_p)^2/(1-x)$. The photon energy spectrum of the lead ion ($Z = 82$), integrated over impact parameter b from $b_{\rm min}$ to infinity, is given by [18]:

$$f_{\gamma/Pb}(x) = \frac{\alpha Z^2}{\pi}\,\frac{1}{x}\left[2x_i K_0(x_i)K_1(x_i) - x_i^2(K_1^2(x_i) - K_0^2(x_i))\right]\,, \tag{2}$$

where $x_i = x\, m_N\, b_{\min}$, and K_0, K_1 are the modified Bessel functions of the second kind of zero and first order, related respectively to the emission of longitudinally and transversely polarized photons. The latter dominating for ultrarelativistic charges ($\gamma \gg 1$). The dominant Higgs decay mode is $\mathrm{H} \to \mathrm{b\bar{b}}$, with a branching fraction of 58% as computed with HDECAY [19]. The PYTHIA8.2 [20] MC generator was employed to shower and hadronize the two final-state b-jets, which are then reconstructed with the Durham k_t algorithm [21] (exclusive 2-jets final-state) using FASTJET 3.0 [22]. The same setup is used to generate the exclusive two-photon production of $b\bar{b}$ and (possibly misidentified) $c\bar{c}$ and light-quark ($q\bar{q}$) jet pairs, which constitute the most important physical background for the measurement of the H$\to b\bar{b}$ channel.

3 Results

The total elastic Higgs boson cross sections in ultraperipheral PbPb and pPb collisions as a function of $\sqrt{s}$ are shown in Fig. 1 (right). We have assigned a conservative 20% uncertainty to the predicted cross sections to cover different charge form factors. At LHC energies, we find a slightly reduced cross section, $\sigma(\mathrm{PbPb} \to \gamma\,\gamma \to \mathrm{H}) = 15 \pm 3$ pb, compared to the results of [8] due a more accurate treatment of the non hadronic-overlap correction based on [23]. The predicted total Higgs boson cross sections are $\sigma(\gamma\,\gamma \to \mathrm{H})$ = 1.75 nb and 1.5 pb in PbPb and pPb collisions at $\sqrt{s_{\mathrm{NN}}}$ = 39 and 63 TeV which, for the nominal $\mathcal{L}_{\mathrm{int}}$ = 110 nb^{-1} and 29 pb^{-1} luminosities per "year" (1-month run), imply ~200 and 45 Higgs bosons produced (corresponding to 110 and 25 bosons in the $b\bar{b}$ decay mode, respectively). The main backgrounds are pairs from the $\gamma\gamma \to b\bar{b}, c\bar{c}, q\bar{q}$ continuum, where charm and light ($q = uds$) quarks are misidentified as b-quarks. The irreducible $\gamma\,\gamma \to b\bar{b}$ background over the mass range $100 < W_{\gamma\,\gamma} < 150$ GeV is ~20 times larger than the signal, but can be suppressed (as well as that from misidentified $c\bar{c}$ and $q\bar{q}$ pairs) via various kinematical cuts. The data analysis follows closely the similar LHC study [8], with the following reconstruction performances assumed: jet reconstruction over $|\eta| < 5$, 7% b-jet energy resolution (resulting in a dijet mass resolution of ~6 GeV at the Higgs peak), 70% b-jet tagging efficiency, and 5% (1.5%) b-jet mistagging probability for a c (light-flavour q) quark. For the double b-jet final-state of interest, these lead to a ~50% efficiency for the MC-generated signal (S), and a total reduction of the misidentified $c\bar{c}$ and $q\bar{q}$ continuum backgrounds (B) by factors of ~400 and ~400 000.

Table 2: Summary of the cross sections and expected number of events per run after event selection criteria (see text) for signal and backgrounds in the $\gamma\,\gamma \to \mathrm{H}(b\bar{b})$ analysis, obtained from events generated with MADGRAPH 5+PYTHIA 8 for PbPb and pPb collisions at FCC energies.

PbPb at $\sqrt{s_{\mathrm{NN}}}$ = 39 TeV	cross section (b-jet (mis)tag efficiency)	visible cross section after $p_T^j, \cos\theta_{jj}, m_{jj}$ cuts	N_{evts} ($\mathcal{L}_{\mathrm{int}}$ = 110 nb^{-1})
$\gamma\,\gamma \to \mathrm{H} \to b\bar{b}$	1.02 nb (0.50 nb)	0.19 nb	21.1
$\gamma\,\gamma \to b\bar{b}$ [$\mathrm{m_{b\bar{b}}}$=100–150 GeV]	24.3 nb (11.9 nb)	0.23 nb	25.7
$\gamma\,\gamma \to c\bar{c}$ [$\mathrm{m_{c\bar{c}}}$=100–150 GeV]	525 nb (1.31 nb)	0.02 nb	2.3
$\gamma\,\gamma \to q\bar{q}$ [$\mathrm{m_{q\bar{q}}}$=100–150 GeV]	590 nb (0.13 nb)	0.002 nb	0.25
pPb at $\sqrt{s_{\mathrm{NN}}}$ = 63 TeV			N_{evts} ($\mathcal{L}_{\mathrm{int}}$ = 29 pb^{-1})
$\gamma\,\gamma \to \mathrm{H} \to b\bar{b}$	0.87 pb (0.42 pb)	0.16 pb	4.8
$\gamma\,\gamma \to b\bar{b}$ [$\mathrm{m_{b\bar{b}}}$=100–150 GeV]	21.8 pb (10.7 pb)	0.22 pb	6.3
$\gamma\,\gamma \to c\bar{c}$ [$\mathrm{m_{c\bar{c}}}$=100–150 GeV]	410. pb (1.03 pb)	0.011 pb	0.3
$\gamma\,\gamma \to q\bar{q}$ [$\mathrm{m_{q\bar{q}}}$=100–150 GeV]	510. pb (0.114 pb)	0.001 pb	0.04

As proposed in [8], various simple kinematical cuts can be applied to enhance the S/B ratio. Since the transverse momenta of the Higgs decay b-jets peak at $p_T^j \approx m_{\mathrm{H}}/2$, selecting events with

at least one jet within p_T = 55–62.5 GeV suppresses $\sim$ 96% of the continuum backgrounds, while removing only half of the signal. Also, one can exploit the fact that the angular distribution of the Higgs decay b-jets in the helicity frame is isotropically distributed in $|\cos\theta_{j_1 j_2}|$, i.e., each jet is independently emitted either in the same direction as the $b\bar{b}$ pair or opposite to it, while the continuum (with quarks propagating in the t- or u- channels) is peaked in the forward–backward directions. Thus, requiring $|\cos\theta_{j_1 j_2}| < 0.5$ further suppresses the continuum contaminations by another $\sim$ 20% while leaving untouched the remaining signal. The significance of the signal can then be computed from the remaining number of counts within 1.4σ around the Gaussian Higgs peak (i.e., $117 < m_{b\bar{b}} < 133$ GeV) over the underlying dijet continuum. Table 2 summarizes the visible cross sections and the number of events after cuts for the nominal luminosities of each system.

In PbPb $\sqrt{s}$ = 39 GeV for the nominal integrated luminosity of $\mathcal{L}_{\rm int} = 110$ nb^{-1} per run, we expect about $\sim$21 signal counts over $\sim$28 for the sum of backgrounds in a window $m_{b\bar{b}}$ = 117–133 GeV around the Higgs peak. Reaching a statistical significance close to 5σ (Fig. 2, left) would require to combine two different experiments (or doubling the luminosity in a single one). Similar estimates for pPb at 63 TeV (29 pb^{-1}) yield about 5 signal events after cuts, over a background of 6.7 continuum events. Reaching a 5σ significance for the observation of $\gamma\,\gamma \to$ H production (Fig. 2, right) would require in this case to run for about 8 months (instead of the nominal 1-month run per year), or running 4 months and combining two experiments. All the derived number of events and significances are based on the aforementioned set of kinematical cuts, and can be likely improved by using a more advanced multivariate analysis.

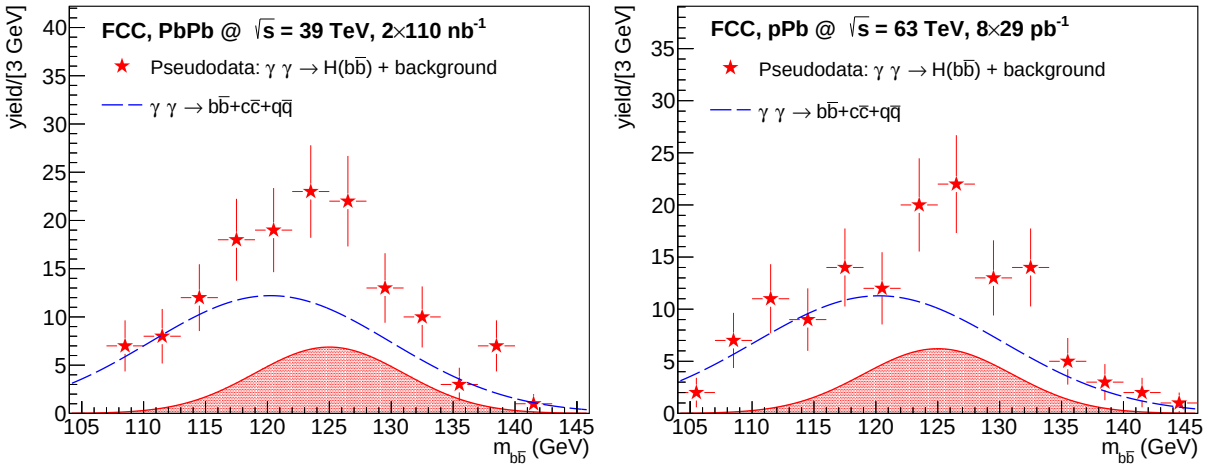

Fig. 2: Expected dijet invariant mass distributions for the combination of photon-fusion Higgs signal (hatched Gaussian) and $b\bar{b} + c\bar{c} + q\bar{q}$ continuum (dashed line) in ultraperipheral PbPb ($\sqrt{s_{\rm NN}} = 39$ TeV, left) and pPb ($\sqrt{s_{\rm NN}} = 63$ TeV, right) collisions, after event selection criteria with the quoted integrated luminosities (see text).

4 Conclusion

We have presented prospect studies for the measurement of the two-photon production of the Higgs boson in the $b\bar{b}$ decay channel in ultraperipheral PbPb and pPb collisions at the FCC. Cross sections have been obtained with MADGRAPH 5, using the Pb (and proton) equivalent photon fluxes and requiring no hadronic overlap of the colliding particles, at nucleon-nucleon c.m. energies of $\sqrt{s_{\rm NN}} = 39$, and 63 TeV. The b-quarks have been showered and hadronized with PYTHIA 8, and reconstructed in a exclusive two-jet final-state with the k_T algorithm. By assuming realistic jet reconstruction performances and (mis)tagging efficiencies, and applying appropriate kinematical cuts on the jet p_T and dijet mass and angles in the helicity frame, we can reconstruct the H($b\bar{b}$) signal on top of the dominant $\gamma\,\gamma \to b\bar{b}$ continuum background. The measurement of $\gamma\,\gamma \to$ H $\to b\bar{b}$ would yield 21 (5) signal counts over 28

(7) continuum dijet pairs around the Higgs peak, in PbPb (pPb) collisions for their nominal integrated luminosities per run. Observation of the photon-fusion Higgs production at the 5σ-level is achievable in the first year by combining the measurements of two experiments (or doubling the luminosity in a single one) in PbPb, and by running for about 8 months (or running 4 months and combining two experiments) in the pPb case. The feasibility studies presented here confirm the interesting Higgs physics potential open to study in $\gamma\gamma$ ultraperipheral ion collisions at the FCC, providing an independent measurement of the H-γ coupling not based on Higgs decays but on a s-channel production mode.

Acknowledgments – P. R. T. acknowledges financial support from the CERN TH Department and from the FCC project.

References

[1] F. Englert, R. Brout, Phys. Rev. Lett. **13** (1964) 321; P. W. Higgs, Phys. Rev. Lett. **13** (1964) 508.

[2] S. Chatrchyan *et al.* [CMS Collaboration], Phys. Lett. B **716** (2012) 30.

[3] G. Aad *et al.* [ATLAS Collaboration], Phys. Lett. B **716** (2012) 1.

[4] D. d'Enterria, PoS ICHEP **2016** (2017) 434 [arXiv:1701.02663 [hep-ex]].

[5] M. L. Mangano *et al.*, CERN Yellow Report **1** (2017), doi:10.23731/CYRM-2017-003.1 [arXiv:1607.01831 [hep-ph]].

[6] A. Dainese *et al.*, CERN Yellow Report **3** (2017) 635, doi:10.23731/CYRM-2017-003.635 [arXiv:1605.01389 [hep-ph]]; and D. d'Enterria *et al.*, QM'17 Proceeds., Nucl. Phys. A **967** (2017) 888 [arXiv:1704.05891 [hep-ex]].

[7] D. d'Enterria, Hard-Probes'16 Proceeds., Nucl. Part. Phys. Proc. **289-290** (2017) 237 [arXiv:1701.08047 [hep-ex]].

[8] D. d'Enterria and J. P. Lansberg, Phys. Rev. D **81** (2010) 014004 [arXiv:0909.3047 [hep-ph]].

[9] C. A. Bertulani and G. Baur, Phys. Rept. **163** (1988) 299.

[10] A. J. Baltz *et al.*, Phys. Rept. **458** (2008) 1 [arXiv:0706.3356 [nucl-ex]]

[11] M. Grabiak *et al.*, J. Phys. G **15** (1989) L25; E. Papageorgiu, Phys. Rev. D **40** (1989) 92; M. Drees *et al.*, Phys. Lett. B**223** (1989) 454; K. J. Abraham *et al.*, Phys. Lett. B **251** (1990) 186.

[12] C. von Weizsäcker *Z. Physik* **88** (1934) 612; E. J. Williams, Phys. Rev. **45** (1934) 729. E. Fermi *Nuovo Cimento* **2** (1925) 143.

[13] S. J. Brodsky, T. Kinoshita and H. Terazawa, Phys. Rev. Lett. **25** (1970) 972; S. J. Brodsky, T. Kinoshita and H. Terazawa, Phys. Rev. D **4** (1971) 1532.

[14] D. d'Enterria, P. Rebello Teles, D.E. Martins, Proceeds. EDS-Blois'17, arXiv:1712.07023 [hep-ph].

[15] J. Alwall *et al.*, JHEP **09** (2007) 028 [arXiv:0706.2334 [hep-ph]].

[16] M. A. Shifman, A. I. Vainshtein, M. B. Voloshin and V. I. Zakharov, Sov. J. Nucl. Phys. **30**, 711 (1979) [Yad. Fiz. **30** (1979) 1368]; B. A. Kniehl and M. Spira, Z. Phys. C **69** (1995) 77; S. Dawson and R. Kauffman, Phys. Rev. D **49** (1994) 2298.

[17] V. M. Budnev, I. F. Ginzburg, G. V. Meledin, V. G. Serbo, Phys. Rept. **15** (1975) 181.

[18] J.D. Jackson, *Classical Electrodynamics*, 2nd edition, John Wiley & Sons (1975).

[19] M. Spira, Nucl. Instrum. Meth. A **389** (1997) 357; A. Djouadi, J. Kalinowski and M. Spira, Comput. Phys. Commun. **108** (1998) 56; A. Djouadi, J. Kalinowski, M. Mühlleitner and M. Spira, arXiv:1003.1643 [hep-ph]; `http://people.web.psi.ch/spira/hdecay/`.

[20] T. Sjöstrand *et al.*, Comput. Phys. Commun. **191** (2015) 159.

[21] S. Catani, Y. L. Dokshitzer, M. H. Seymour and B. R. Webber, Nucl. Phys. B **406** (1993) 187.

[22] M. Cacciari, G. P. Salam and G. Soyez, Eur. Phys. J. C **72** (2012) 1896 [arXiv:1111.6097 [hep-ph]].

[23] S. R. Klein *et al.*, Comput. Phys. Commun. **212** (2017) 258 [arXiv:1607.03838 [hep-ph]].